Journal of Sound and Vibration (1997) **199**(2), 165–175

THE COEXISTENCE OF PERIODIC, ALMOST-PERIODIC AND CHAOTIC ATTRACTORS IN THE VAN DER POL–DUFFING OSCILLATOR

W. Szemplińska-Stupnicka and J. Rudowski

Institute of Fundamental Technological Research, Polish Academy of Sciences, Świętokrzyska 21, 00-049 *Warsaw, Poland*

(*Received* 16 *June* 1995, *and in final form* 3 *January* 1996)

In this paper are presented the computer simulation and the approximate theoretical analysis of the behaviour of the van der Pol–Duffing forced oscillator at the passage through principal resonance, at increasing and decreasing driving frequency. Almost-periodic oscillations, frequency locking, transition to chaotic motion and the jump from the non-resonant to the resonant state are observed and interpreted in the light of approximate analytical theory and by the use of topological concepts.

1. INTRODUCTION

The classic van der Pol forced system governed by the equation

$$\ddot{x} - \mu(1 - x^2)\dot{x} + \Omega_0^2 x + f(x, t) = 0, \tag{1}$$

which serves as a basic model of self-excited oscillations in physics, mechanics, biology, electronics, chemistry and many other disciplines, has been studied intensively since 1927 [1–9]. Recent analysis has been focused on the generation of chaotic motion in the system provided with cubic non-linearity and driven by a harmonic force [10–16]:

$$\ddot{x} - \mu(1 - x^2)\dot{x} + \Omega_0^2 x + \alpha x^3 - F\cos \nu t = 0, \qquad T = 2\pi/\nu. \tag{2}$$

The system (2) was considered by the authors in reference [17], but the study was confined to the region of driving frequency which is close to and below the principal resonance (principal resonance occurs when ν is close to the frequency of the limit cycle of the system (2) for $F = 0$). Transition from T-periodic resonant motion through a chaotic motion zone to almost-periodic oscillations was observed and interpreted in terms of Neimark bifurcations.

In this paper we continue the study of the system (2), but consider the phenomena which occur at the passage through the principal resonance. As the frequency increases the system reaches the saddle-node bifurcation point of the T-periodic solution and, after transients, settles down into the non-resonant state. The non-resonant state, which coexists with the resonant solution in a certain frequency interval, shows very rich behaviour. The non-resonant almost-periodic oscillation, frequency locking, the passage through a chaotic motion zone and the jump back on to the resonant solution at decreasing frequency are the main points considered in this paper.

0022–460X/97/020165 + 11 $25.00/0/sv960648

First, in section 2 we overview the approximate theoretical analysis of the instability of the T-periodic solution and focus on the result which applies to the "post-resonance" frequency region to be considered.

Then, in section 3, the system behaviour at the passage through the principal resonance is illustrated by computer simulation analysis. Various bifurcations for increasing and decreasing driving frequency are observed and interpreted in terms of frequency spectra and Poincaré maps of the steady state responses. The transition from the discrete frequency spectrum of the almost-periodic solution, via "periodic windows" (frequency locking), up to the continuous type spectrum representing chaotic motion is studied in detail.

In section 4 some attempts are made towards theoretical approximate analysis of the multi-frequency, almost-periodic response. It is found that, despite the fact that the frequencies involved in the solution are very close to commensurable values, and even are commensurable in frequency locking intervals, the harmonic balance method is capable of capturing the essence of the complex, multi-frequency solution.

Finally, the hysteresis behaviour, the sudden destruction of the chaotic attractor and the jump from non-resonant to resonant motion are discussed.

2. INSTABILITY AND BIFURCATIONS OF THE HARMONIC SOLUTION

It is known that the principal resonance, where the driving frequency is close to the limit-cycle frequency, the steady state response of the system becomes T-periodic and is close to being a harmonic function of time [3]:

$$x(t) = C\cos(vt + \varphi) \equiv x(t + T), \qquad T = 2\pi/v. \tag{3}$$

The amplitude curves of the approximate solution can be obtained by any of the commonly accepted approximate methods—averaging, harmonic balance, asymptotic or multiple-scales method [17, 18]—with the result

$$C = F/\sqrt{[\Omega^2(C) - v^2]^2 + \mu^2 v^2[1 - C^2/4]^2}, \tag{4a}$$

$$\tan\varphi = \mu v(1 - \tfrac{1}{4}C^2)/[\Omega^2(C) - v^2], \qquad \Omega^2(C) = \Omega_0^2 + \tfrac{3}{4}\alpha C^2. \tag{4b}$$

Analogously the limit-cycle oscillation in the autonomous system (2) for $F = 0$ is also assumed to be a harmonic function of time,

$$x_{F=0}(t) = a\cos\omega_0 t, \tag{5}$$

and the approximate calculations yield

$$a = 2, \qquad \omega_0 = \sqrt{\Omega_0^2 + \tfrac{3}{4}\alpha a^2}. \tag{6a}$$

At $\Omega_0 = 0$ and $\alpha = 1$ one obtains $\omega_0 = \sqrt{3} \simeq 1{\cdot}73$. The approximation seems to be adequate, because the computer simulations give

$$a \simeq 1{\cdot}81, \qquad \omega_0 \simeq 1{\cdot}625, \qquad \mu = 0{\cdot}2. \tag{6b}$$

The local stability of the harmonic solution (3) is now examined by adding a small disturbance,

$$\bar{x} = x(t) + \delta x, \tag{7}$$

where $x(t)$ represents the steady state solution with $C = \text{constant}$, $\varphi = \text{constant}$ and considering the linear variational equation for $\delta x(t)$,

$$\delta\ddot{x} + \delta x G(t) + \delta\dot{x}R(t) = 0, \tag{8}$$

where $G(t)$ and $R(t)$ are periodic functions of time [3, 17, 18]:

$$G(t) = G(t + T/2), \qquad R(t) = R(t + T/2).$$

On introducing a new variable η, by setting

$$\delta x(t) = \eta(t) \exp\left[-\int_0^t \tfrac{1}{2} R(\tau)\, \mathrm{d}\tau \right] \equiv \eta(t)\, \mathrm{e}^{[-\delta t - p(t)]}, \tag{9}$$

where $p(t) = (\mu C^2)/(8v) \sin(2vt)$, the variational equation (8) is reduced to the Hill-type equation

$$\ddot{\eta} + \eta G_1(t) = 0, \qquad G_1(t) = G_1(t + T/2), \tag{10}$$

and this enables one to apply the Floquet theorem. Confining attention to the first order instability one can apply the first approximate solution as [3, 18]

$$\eta(t) = \mathrm{e}^{\varepsilon_{1,2} t} \cos(vt + \beta), \tag{11}$$

where $\varepsilon_{1,2}$, due to the Floquet theory, can be real or imaginary, but not complex. The solution for $\eta(t)$ is unstable if $\varepsilon_{1,2}$ are real, because they satisfy the conditions $\varepsilon_1 > 0$ and $\varepsilon_2 < 0$, and is stable if $\varepsilon_{1,2}$ are purely imaginary. The variation $\delta x(t)$ may, however, exhibit an additional form of instability because equation (9) yields

$$\delta x(t) = \eta(t)\, \mathrm{e}^{(-\delta t - p(t))} \simeq \mathrm{e}^{(\varepsilon_{1,2} - \delta)t} \cos(vt + \beta), \tag{12a}$$

and δ can be positive or negative:

$$\delta = (\mu/2)[(C^2/2) - 1], \qquad \delta < 0 \quad \text{if} \quad C < \sqrt{2}. \tag{12b}$$

At negative values of the coefficient δ and purely imaginary $\varepsilon_{1,2}$ the solution for $\delta x(t)$ becomes unstable.

The periodic function of time $p(t)$ is ignored in the further analysis, because it does not affect the stability question.

To sum up, the system may develop two forms of instability as follows.

I. The classic instability is characterized by real and positive values of the exponent ε, $\delta > 0$ and $\varepsilon^2 > \delta^2$. The region is easily identified on the amplitude curve: the unstable portions of $C \equiv C(v)$ are those which satisfy the condition that $\Omega^2(C) - v^2$ and $\mathrm{d}C/\mathrm{d}v$ have opposite signs. The instability limits coincide with the points on the amplitude curves which have vertical tangents. The unstable solution for the disturbance $\delta x(t)$ in the region can be written as (see equation 12(a))

$$\delta x(t)_u = \mathrm{e}^{(-\delta + \varepsilon_1)t} \cos(vt + \delta), \tag{13}$$

where it is assumed that $\varepsilon_1 > 0$ and $\varepsilon_2 < 0$, and therefore $-\delta + \varepsilon_1 > 0$ and the amplitude of the harmonic term grows exponentially.

II. The Neimark type instability is characterized by imaginary values of the exponent ε in equations (11): $\varepsilon_{1,2} = \pm \mathrm{i}\bar{\varepsilon}$, $\bar{\varepsilon}$ real, and negative values of the parameter $\delta(C)$: $\delta(C) < 0$; that is $C < \sqrt{2}$. The two conditions result in solutions for the disturbance $\delta x(t)$ which develop almost-periodic oscillations with the amplitude growing in time:

$$\delta x(t) = \mathrm{e}^{(-\delta \pm \mathrm{i}\bar{\varepsilon})t} \cos(vt + \beta),$$

$$\delta x(t) = \mathrm{e}^{-\delta t}\{B_1 \cos[(v + \bar{\varepsilon})t + \theta_1] + B_2 \cos[(v - \bar{\varepsilon})t + \theta_2]\}, \tag{14}$$

where $-\delta > 0$, and $v + \bar{\varepsilon}$ and $v - \bar{\varepsilon}$ are incommensurate frequencies.

The two unstable regions are depicted in Figure 1. It is clear that the portion of amplitude curve between the points D_1 and D_2 is unstable in the sense of criterion I and that point B is the Neimark bifurcation point, i.e., the branch AB is unstable in the sense of criterion II.

In the region in which the two forms of unstable regions overlap (branch E–D_2 in Figure 1), both conditions of instability are satisfied: i.e., $\varepsilon_{1,2}$ are real and $\delta(C)$ is negative. Therefore, the solution for the disturbance $\delta x(t)$ has the same form as that in the region I (equation (13): that is, the instability of the harmonic solution manifests itself by the exponential growth of the amplitude of the harmonic term. Note, however, that now the amplitude grows "faster", because both components in the exponential term, $-\delta$ and ε_1, are positive.

It follows that in the region of the driving frequency considered in Figure 1 only the upper, resonant branch B–D_1 of the harmonic solution (3) is stable; the remaining branch D_1–E–D_2–G is unstable. The fact that the branch D_2–G is unstable in the Neimark sense (equation (14)) gives strong indications that one may expect almost-periodic solutions to occur in the region.

3. COMPUTER SIMULATION ANALYSIS

In this section an investigation of the almost-periodic non-resonant oscillations by computer simulation (numerical experiment) is described. The computation was performed in a quasi-static manner. For fixed values of the driving force and the damping term, the driving frequency ω was gradually changed by a small step $\Delta\omega$. The initial conditions for the "next step" frequency $\omega_{i+1} = \omega_i + \Delta\omega$ corresponded to the steady state solution for the previous frequency ω_i. In this way the duration of the transient motion was considerably reduced. The frequency step $\Delta\omega$ and the number of cycles ignored in the computation to allow the transient to decay was adapted to the sensitivity of the response to the change of parameters. The driving frequency ω was either decreased or increased to explore the hysteresis behaviour of the system. The possibility of existence of any other attractors was ruled out by starting the computation with a set of various initial conditions.

In Figure 2 are depicted the theoretical amplitude curve $C = C(\nu)$ and the amplitudes of harmonic components obtained by computer simulations in the resonant and non-resonant state.

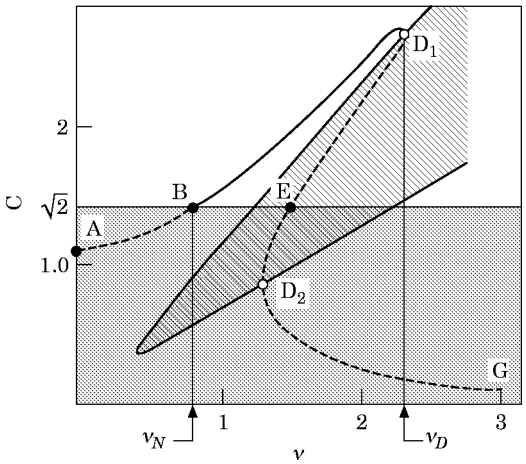

Figure 1. Amplitude curves and unstable regions of the harmonic solution: $F = 1{\cdot}0$, $\mu = 0{\cdot}2$.

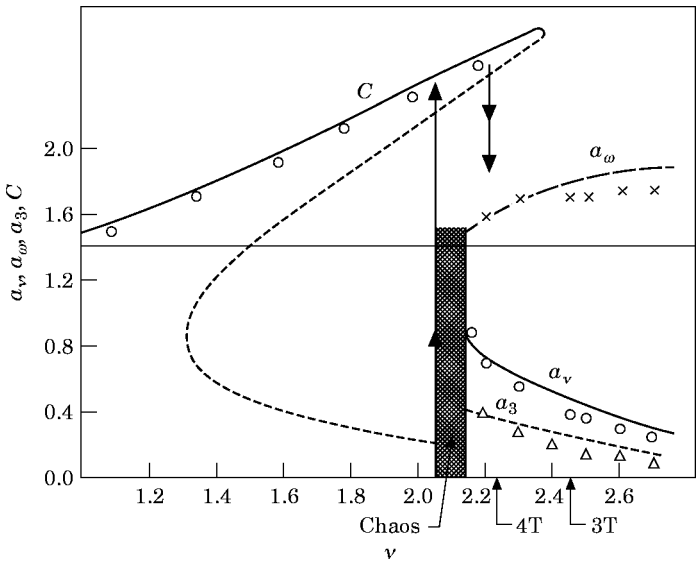

Figure 2. Amplitude curves of the harmonic and almost-periodic solutions: theoretical and computer simulation results: ——, ○○○, a_v, amplitude of the frequency v harmonic component; — — —, × × × ×, a_ω, amplitude of the forced limit cycle with frequency ω (for ω, see Figure 6); ----, △△△△, a_3, amplitude of the harmonic component with the frequency $2\omega - v$.

In Figures 3–5 are illustrated three different responses observed beyond the principal resonance: almost-periodic (Figure 3), periodic (Figures 4(a) and 4(b)) and chaotic (Figure 5). Non-resonant solutions exist at driving frequencies higher than $v \simeq 2{\cdot}05$. One sees that in the frequency spectrum of the almost-periodic and periodic solutions there is one dominating harmonic component with frequency denoted by ω. The frequency varies slightly with v but remains very close to the limit-cycle frequency of the autonomous system ($\omega_0 \simeq 1{\cdot}625$).

The two other harmonic components which have considerable amplitudes are a_v, with the frequency of the driving force, and a_3, with the combination frequency $\omega_3 = 2\omega - v$. Variations of the "forced limit-cycle" frequency ω, the ratio ω/v and the combination frequency $2\omega - v$ with frequency v are depicted in Figure 6.

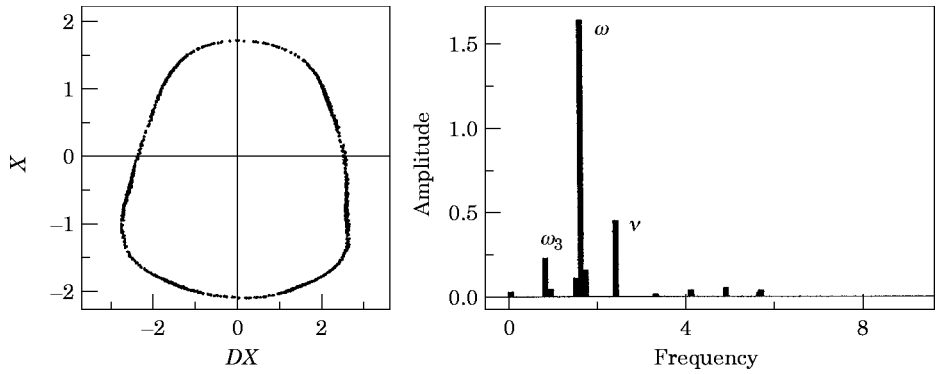

Figure 3. The Poincaré map and frequency spectrum of the almost-periodic oscillations: $\mu = 0{\cdot}2$, $F = 1{\cdot}0$, $v = 2{\cdot}40$.

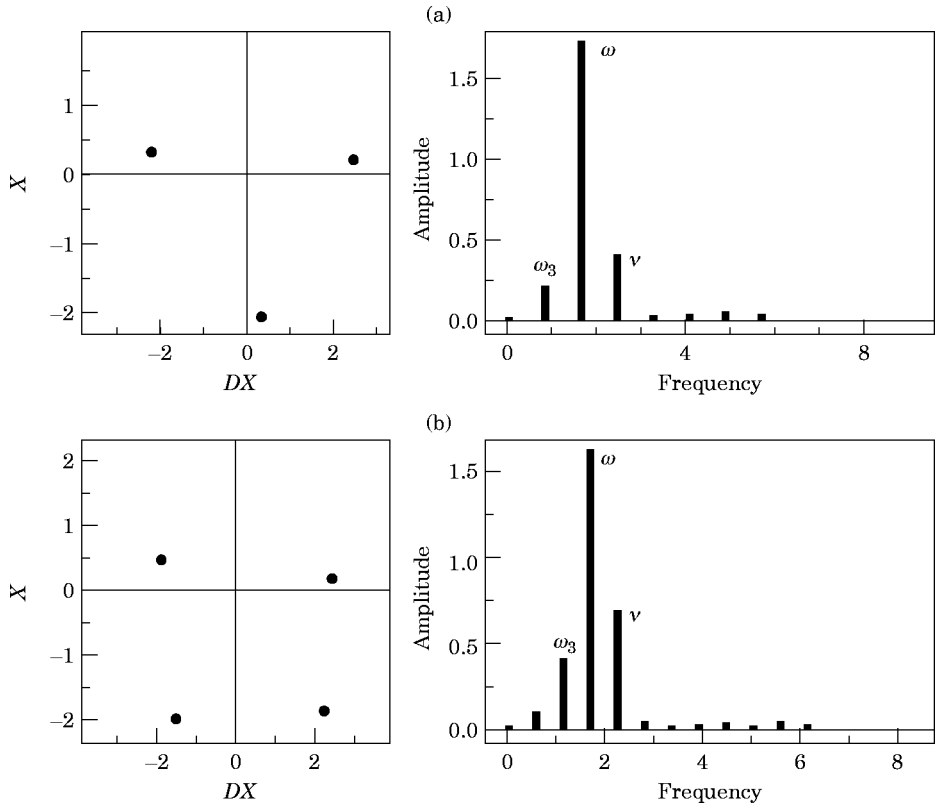

Figure 4. The Poincaré map and frequency spectrum of periodic solutions: $F = 1{\cdot}0$, $\mu = 0{\cdot}2$. (a) 3T-periodic oscillations, $\nu = 2{\cdot}45$; (b) 4T-periodic oscillations, $\nu = 2{\cdot}23$.

Within the zone of the driving frequency $2{\cdot}05 < \nu < 2{\cdot}21$ the resonant state coexists with the T-periodic high amplitude resonant motion. While the higher frequency boundary of the region $\nu = 2{\cdot}21$ is close to the classic saddle-node bifurcation point of the harmonic solution (3), the lower frequency limit does not coincide with any bifurcation point of periodic solution and differs considerably from the other point with vertical tangent on the theoretical amplitude curve $C(\nu)$. This is not a surprise, since point D_2 in Figure 1 does

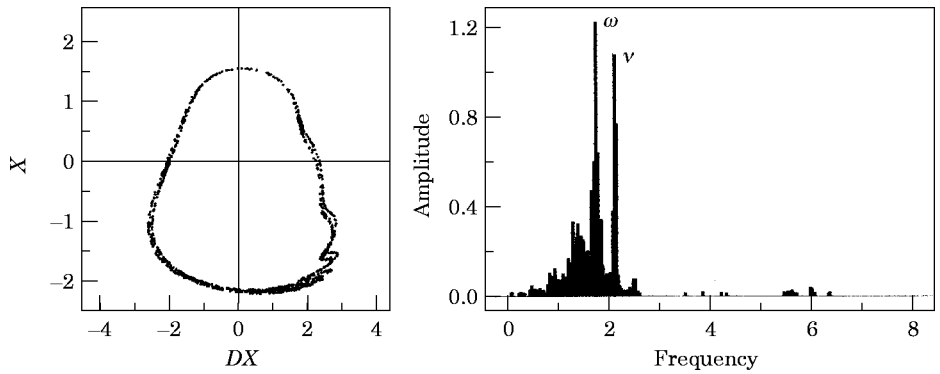

Figure 5. The Poincaré map (strange attractor) and frequency spectrum of chaotic motion: $F = 1{\cdot}0$, $\mu = 0{\cdot}2$.

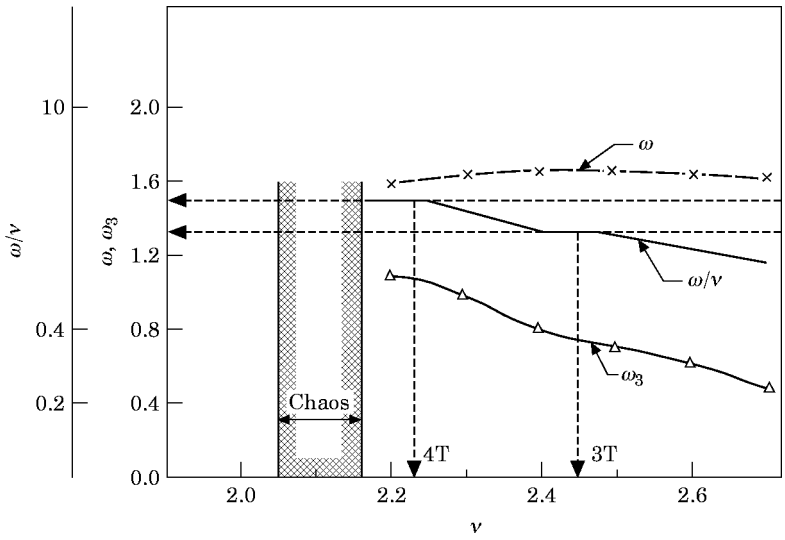

Figure 6. Variations of frequencies in the almost-periodic oscillations: computer simulation results.

not play here a role of stability limit: the whole branch of the amplitude curve D_1–E–D_2–G is unstable.

The resonant motion characteristics, which are plotted in Figures 3–5 and are observed at decreasing frequency, lead to the following observations.

As ν decreases, the frequencies of the three dominating harmonic components approach each other and the ratio ω/ν grows from the value $\omega/\nu \simeq 0{\cdot}58$ at $\nu = 2{\cdot}7$ to $\omega/\nu \simeq 0{\cdot}78$ at $\nu = 2{\cdot}18$.

In the frequency region considered there occur two frequency locking zones: in the neighbourhood of $\nu = 2{\cdot}45$ the ratio is $\omega/\nu = \frac{2}{3}$, so that the response is 3T-periodic (see Figure 4(a)). In the vicinity of $\nu = 2{\cdot}23$ the ratio reaches the value $\omega/\nu = \frac{3}{4}$ and the resulting motion is 4T-periodic (see Figure 4(b)).

Below $\nu = 2{\cdot}2$ the discrete frequency spectrum condenses and gradually gains a continuous type character. Thus the motion transforms continuously into a chaotic one and the chaotic state is sustained within a narrow strip on the frequency axis (see Figures 2, 5 and 6).

The chaotic attractor disappears suddenly at $\nu \simeq 2{\cdot}05$ and the system response, after some transient, jumps up to the resonant T-periodic solution. It follows that at frequencies below $\nu = 2{\cdot}05$ the resonant motion is a unique attractor of the system (until the Neimark instability at point B in Figure 1).

The motion illustrated in Figure 5 has been called "chaotic". One may have doubts about it, because, at first glance, it does not differ much from almost-periodic oscillations. To determine whether or not the response is chaotic, we calculated maximal Lyapunov exponent, with the result $\sigma_{max} = 0{\cdot}05 > 0$. Thus there is no doubt that the response falls into the category of chaotic motion.

We can interpret and explain the metamorphoses of the non-resonant response with variation of the frequency ν from the point of view of the concept of frequency locking. We deal here with two fundamental frequencies: the "forced limit cycle frequency" ω and the driving frequency ν. The former remains almost constant while the latter is decreasing, so that the ratio ω/ν varies. The two types of frequency locking observed, $\omega/\nu = \frac{2}{3}$ and

$\omega/v = \frac{3}{4}$ (see Figure 6) are reached in a smooth, continuous way, and the corresponding amplitudes a_ω and a_v do not undergo sudden jumps.

At a further decrease of the driving frequency v the ratio ω/v further increases and at $\omega/v \simeq 1{\cdot}55$ the response undergoes dramatic changes: first the motion becomes chaotic (see Figure 6) and then a sudden destruction of the chaotic attractor and a jump to the T-periodic motion, i.e., to the response with the frequency locking $\omega/v = 1$, is observed.

The sudden destruction of the chaotic attractor can be also explained in terms of the concept of "boundary crisis" [19]. As v decreases, the saddle point of the T-periodic resonant solution approaches the non-resonant attractor and finally collides with it. From the topological point of view this corresponds to the critical situation when the stable and unstable manifolds of the saddle point become tangent, and then intersect with each other [20]. In this way the domain of attraction of the non-resonant motion ceases to exist, and the T-periodic resonant attractor becomes globally stable.

4. THEORETICAL NON-RESONANT ALMOST-PERIODIC SOLUTION

It is known that in the literature on non-linear oscillations and on approximate analytical methods one can hardly find a clear indication as to how to determine an almost-periodic solution in the van der Pol–Duffing system, the solution of which would give satisfactory agreement with the computer simulation [3, 16].

First, we tried several perturbation techniques, seeking for a method which leads to reasonable, satisfactory results within a low order approximation. Finally, we concluded that perturbation methods are not adequate for our problem. The trouble begins at an early stage of application of the procedure. To obtain satisfactory results in the first or second approximation, one has to find an approximate zero order solution to be perturbed. The question is how to find it. The assumption that the zero order approximate solution is a superposition of the limit cycle of autonomous system and forced oscillations of the linear system does not lead to satisfactory results.

Therefore we turned to another category of approximate analytical method, the category which does not make use of the idea of a "small parameter", but requires some assumptions about the form of the solution as a function of time. If periodic solutions are considered, the methods are reduced to the Ritz or Galerkin methods [16, 18]. The procedure is often called "harmonic balance" and it can be extended to the almost-periodic solution. Here we apply the generalized harmonic balance principle for the solution, which is assumed to consist of three harmonic components,

$$x(t) = a_v \cos(vt + \varphi) + a \cos\theta + a_3 \cos\psi, \tag{15a}$$

where $\theta = \omega t$ and $\psi = (2\omega - v)t + \phi$. The solution involves six unknown coefficients to be determined:

$$a_v, a, a_3, \varphi, \omega, \phi. \tag{15b}$$

Following the harmonic balance rule we insert the approximate solution (15a) into equation of motion (2). The residual thus obtained is denoted as $\varepsilon(t)$. Then we apply the generalized orthogonality condition of the Galerkin method [16, 18]:

$$\lim_{T\to\infty} \frac{1}{T} \int_0^T \varepsilon(t) \cos(\beta_i t)\, \mathrm{d}t = 0, \quad \lim_{T\to\infty} \frac{1}{T} \int_0^T \varepsilon(t) \sin(\beta_i t)\, \mathrm{d}t = 0, \qquad i = 1, 2, 3,$$

$$\beta_1 \equiv v, \qquad \beta_2 \equiv \omega, \qquad \beta_3 \equiv 2\omega - v. \tag{16}$$

The condition (16) can be interpreted as the "harmonic balance principle", because, in fact, they impose the following procedure: expand the residual $\varepsilon(t)$ into a generalized Fourier series; then equate to zero separately coefficients of the three harmonic components involved in the assumed solution (15a) and ignore all other remaining harmonics.

The procedure defined by equation (16) leads to the desired six equations for the unknown amplitude, frequency and phase angles (15b). To derive the equation correctly one has to consider the problem of "combination tones", which are involved in the generalized Fourier series of the residual $\varepsilon(t)$.

Note, that due to the almost-periodic nature of the solution (15a), the residual involves combination harmonics with the frequencies $r_1\omega + r_2 v$, where r_1 and r_2 are integers. In the procedure applied here, one assumes that none of the combination tones involved in the residual $\varepsilon(t)$ produces additional terms into the harmonic balance equation (16): i.e.,

$$r_1\omega + r_2 v \neq v \qquad \text{and} \qquad r_1\omega + r_2 v \neq \omega. \tag{17}$$

One may have doubts about the assumption, because in fact the two frequencies become rational within the range of driving frequency under consideration. We know that we are supposed to take into account the relations $\omega/v = \frac{2}{3}$ and $\omega/v = \frac{3}{4}$. Therefore we have to answer the question of whether the harmonic balance equations apply to both types of response, i.e., almost-periodic and periodic, at the ratios $\omega/v = \frac{2}{3}$ and $\omega/v = \frac{3}{4}$. If not, different equations should be derived for calculations of the amplitude curves at the frequency locking intervals.

We checked the problem carefully, considering the combination tones involved in the residual. Our conclusion is that at the frequency locking $\omega/v = \frac{3}{4}$ all of the combination type harmonics satisfy relations (17). At the ratio $\omega/v = \frac{2}{3}$, however, the harmonic components of the type

$$\sin 3\psi \equiv \sin[(6\omega - 3v)t + \phi] \tag{18}$$

appear to bring new coefficients into two of the six harmonic balance equations (16): that is, produce additional coefficients of harmonic components $\cos vt$ and $\sin vt$:

$$\lim_{T\to\infty} \frac{1}{T}\int_0^T \varepsilon(t)\cos vt\, \mathrm{d}t = 0, \qquad \lim_{T\to\infty} \frac{1}{T}\int_0^T \varepsilon(t)\sin vt\, \mathrm{d}t = 0. \tag{19}$$

We find the additional terms immediately when we eliminate ω in the equation (18) by setting $\omega = \frac{2}{3}v$:

$$\sin 3\psi \equiv \sin[(6\omega - 3v)t + \phi] = \sin(vt + \phi) = \sin vt\cos\phi + \cos vt\sin\phi. \tag{20}$$

We also find that the amplitude of this harmonic component in the residual is small, of order a_3^3, and that the additional terms in the harmonic balance equation do not bring observable effects into the solution for a, a_v and a_3.

Therefore, we apply the harmonic balance method under the assumption that the frequencies involved are incommensurate. The equations (16) are reduced to the form

(1) $$-\omega^2 + \tfrac{3}{4}a^2 + \tfrac{3}{2}a_v^2 + \tfrac{3}{2}a_3^2 + \tfrac{1}{2}a_v a_3[3\cos\phi + \mu(\omega - v)\sin\phi] = 0,$$

(2) $$\mu\omega(1 - \tfrac{1}{4}a^2 - \tfrac{1}{2}a_v^2 - \tfrac{1}{2}a_3^2) - \tfrac{1}{2}a_v a_3[3\sin\phi + \mu(\omega - v)\cos\phi] = 0,$$

(3) $$-v^2 a_v + \tfrac{3}{4}a_v^3 + \tfrac{3}{2}a_v a^2 + \tfrac{3}{2}a_v a_3^2 + \tfrac{1}{4}a^2 a_3[3\cos\phi + \mu v\sin\phi] - F\cos\varphi = 0,$$

(4) $$\mu a_v v(1 - \tfrac{1}{4}a_v^2 - \tfrac{1}{2}a^2 - \tfrac{1}{2}a_3^2) + \tfrac{1}{4}a^2 a_3[3\sin\phi - \mu v\cos\phi] - F\sin\varphi = 0,$$

$$-a_3(2\omega - v)^2 + \tfrac{3}{2}a_3(\tfrac{1}{2}a_3^2 + a^2 + a_v^2) + \tfrac{1}{4}a^2 a_v[3\cos\phi + \mu(2\omega - v)\sin\phi] = 0, \tag{5}$$

$$\mu a_3(2\omega - v)(1 - \tfrac{1}{2}a^2 - \tfrac{1}{2}a_v^2 - \tfrac{1}{4}a_3^2) + \tfrac{1}{4}a^2 a_v[3\sin\phi - \mu(2\omega - v)\cos\phi] = 0. \tag{6}$$

(21)

Equations (21) form a set of six algebraic–trigonometric non-linear equations for six unknowns: a_v, a, a_3, φ, ω and ϕ. On solving them one obtains the amplitude curves sought: that is, the unknown parameters are functions of the driving frequency v. The results are plotted in Figure 2 together with the amplitudes a_v, a and a_3 determined by computer simulation analysis. A comparison of the theoretical and computer simulation results reveals that the theoretical calculations give a reasonable approximation. One may even argue that the simple approximate method fails. In any case, we observed a good qualitative coincidence and satisfactory estimates of the amplitude curves. This signals that the simple approximate three-harmonic solution captures the essence of the complex, multi-frequency response of the non-resonant response.

5. CONCLUSIONS

The computer simulations and the theoretical approximate analysis of the van der Pol–Duffing forced oscillator in the close neighbourhood of the principal resonance can be summed up as follows.

The Neimark type instability of harmonic solution obtained by first order approximate analysis is a strong indicator for almost-periodic solutions to occur.

The non-resonant response in the neighbourhood of the principal resonance reveals very complex behaviour: almost-periodic, periodic and chaotic motion appears as the driving frequency varies.

The two steady states, resonant and non-resonant, coexist within a range of frequencies, but the range is much smaller than that in the dissipative Duffing system.

The jump from non-resonant to resonant oscillations is preceded by a chaotic motion region; thus one may interpret chaotic motion as a transition state between multi-frequency, almost-periodic non-resonant motion and the T-periodic, nearly harmonic resonant oscillations.

The jump from the non-resonant to the resonant state is not related to any local bifurcation of the periodic solution; one can interpret the sudden destruction of the chaotic attractor by the use of the concepts of topological methods. Our observations and experience give strong indicators that this is the scenario of the boundary crisis (collision of the chaotic attractor with the saddle associated with the harmonic T-periodic solution) that occurs at the lower frequency boundary of the chaotic region.

REFERENCES

1. B. VAN DER POL 1927 *Philosophical Magazine* **7**, 65–80. Forced oscillations in a system with nonlinear resistance.
2. J. J. STOCKER 1950 *Nonlinear Vibrations in Mechanical and Electrical Systems*. New York: Interscience.
3. CH. HAYASHI 1984 *Nonlinear Oscillations in Physical Systems*. Princeton, NJ: Princeton University Press.
4. J. GUCKENHEIMER and P. HOLMES 1983 *Nonlinear Oscillations, Dynamical Systems and Bifurcations of Vector Fields*. New York: Springer-Verlag.
5. T. ENDO and T. SAITO 1990 *Transactions of the IEICE* **E73**, 763–771. Chaos in electrical and electronic circuits and systems.
6. U. PARLITZ and W. LAUTERBORN 1987 *Physical Review A* **36**, 1428–1434. Period-doubling cascade and devil's staircase of the driven van der Pol oscillator.

7. G. Quin, D. Dong, R. Li and X. Wen 1989 *Physics Letters A* **141,** 412–416. Rich bifurcation behaviors of the driven van der Pol oscillator.
8. A. B. Belogortsev, D. M. Vavriv and O. A. Tretyakov 1993 *Applied Mechanics Review* **46**, 372–384. Destruction of quasiperiodic oscillations in weakly nonlinear systems.
9. J. Brindley, T. Kapitaniak and M. S. El Naschie 1991 *Physica D* **51**, 28–38. Analytical conditions for strange chaotic and nonchaotic attractors of the quasiperiodically forced van der Pol equation.
10. Y. Ueda and N. Akamatsu 1981 *IEEE Transactions on Circuits and Systems* **CAS-28,** 217–223. Chaotically transitional phenomena in the forced negative-resistance oscillator.
11. H. Kawakami and Ch. Hayashi 1981 26 *Internation Wissenschaft Colloquium TH Ilmenau*. Bifurcation and chaotic states of the solution of Duffing–van der Pol equation.
12. A. S. Dimitriev, W. A. Kishov and A. G. Spiro 1983 *Radiotechnika i Elektronika* **12**, 2430–2439. Chaotic oscillations in nonautonomous with reactive nonlinearity (in Russian).
13. D. K. Arrowsmith and K. J. Taha 1983 *Meccanica* **18**, 195–204. Bifurcations of a particular forced van der Pol oscillator.
14. W.-H. Steeb and A. Kunick 1987 *International Journal of Non-linear Mechanics* **22**, 349–361. Chaos in limit cycle systems with external periodic excitation.
15. A. S. Dimitriev, U. A. Komlev and D. V. Turaev 1992 *International Journal of Bifurcation and Chaos* **2**, 93–100. Bifurcation phenomena in the 1–1 horn for the forced van der Pol–Duffing system.
16. L. V. Kantorowitch and V. T. Krylov V. 1958 *Approximate Methods of Higher Analysis*. New York: Interscience.
17. W. Szemplińska-Stupnicka and J. Rudowski 1994 *Physics Letters A* **192**, 201–206. Neimark bifurcation, almost-periodicity and chaos in the forced van der Pol–Duffing system in the neighbourhood of the principal resonance.
18. W. Szemplińska-Stupnicka 1990 *The Behaviour of Nonlinear Vibrating Systems*. Dordrecht: Kluwer Academic.
19. C. Grebogi, E. Ott and J. A. Yorke 1983 *Physica D* **7**, 181–200. Crisis, sudden changes in chaotic attractors and transient chaos.
20. E. Ott 1993 *Chaos in Dynamical Systems*. Cambridge: Cambridge University Press.